SIAM/ASA J. Uncertainty Quantification
Vol. 3, pp. 709–736

Probabilistic Description of Extreme Events in Intermittently Unstable Dynamical Systems Excited by Correlated Stochastic Processes*

Mustafa A. Mohamad† and Themistoklis P. Sapsis†

Abstract. In this work, we consider systems that are subjected to intermittent instabilities due to external stochastic excitation. These intermittent instabilities, though rare, have a large impact on the probabilistic response of the system and give rise to heavy-tailed probability distributions. By making appropriate assumptions on the form of these instabilities, which are valid for a broad range of systems, we formulate a method for the analytical approximation of the probability distribution function (pdf) of the system response (both the main probability mass and the heavy-tail structure). In particular, this method relies on conditioning the probability density of the response on the occurrence of an instability and the separate analysis of the two states of the system, the unstable and stable states. In the stable regime we employ steady state assumptions, which lead to the derivation of the conditional response pdf using standard methods for random dynamical systems. The unstable regime is inherently transient, and in order to analyze this regime we characterize the statistics under the assumption of an exponential growth phase and a subsequent decay phase until the system is brought back to the stable attractor. The method we present allows us to capture the statistics associated with the dynamics that give rise to heavy-tails in the system response, and the analytical approximations compare favorably with direct Monte Carlo simulations, which we illustrate for two prototype intermittent systems: an intermittently unstable mechanical oscillator excited by correlated multiplicative noise and a complex mode in a turbulent signal with fixed frequency, where nonlinear mode interaction terms are replaced by a stochastic drag and additive white noise forcing.

Key words. heavy-tails, rare events, uncertainty quantification, intermittent instabilities, correlated excitation

AMS subject classifications. 62G32, 60H10, 60H30, 60H35, 34F05

DOI. 10.1137/140978235

1. Introduction.

A wide range of dynamical systems describing physical and technological processes is characterized by intermittency, i.e., the property of having sporadic responses of extreme magnitude when the system is "pushed" away from its statistical equilibrium. This intermittent response is usually formulated through the interplay of stochastic excitation, which can trigger internal system instabilities, deterministic restoring forces (usually in terms of a potential), and dissipation terms. The result of intermittent instabilities can be observed by the heavy-tails in the statistics of the system response. It is often the case that, despite the high dimensionality of the stable attractor, where the system resides most of the time, an extreme response of short duration is due to an intermittent instability occurring over a single mode. This scenario does not exclude the case of having more than one intermittent mode

*Received by the editors July 21, 2014; accepted for publication (in revised form) June 29, 2015; published electronically August 18, 2015. This research has been partially supported by the Naval Engineering Education Center (NEEC) grant 3002883706 and by the Office of Naval Research (ONR) grant ONR N00014-14-1-0520.
http://www.siam.org/journals/juq/3/97823.html

†Department of Mechanical Engineering, Massachusetts Institute of Technology, Cambridge, MA 02139 (mmohamad@mit.edu, sapsis@mit.edu).

as long as the extreme responses of these modes are statistically independent. For this case, it may be possible to analytically approximate the probabilistic structure of these modes and understand the effect of the unstable dynamics on the heavy-tails of the response.

Instabilities of this kind are common in dynamical systems with uncertainty. One of the most popular examples is modes in turbulent fluid flows and nonlinear water waves subjected to nonlinear energy exchanges that occur in an intermittent fashion and result in intermittent responses [1, 2, 3, 4, 5, 6, 7]. Prototype systems that mimic these properties were introduced in [8, 9, 10]. In recent works, it has been shown that properly designed single mode models can describe intermittent responses, even in very complex systems characterized by high dimensional attractors [10, 11, 12]. Another broad class of such systems includes mechanical configurations subjected to parametric excitations, such as the parametric resonance of oscillators and ship rolling motion [13, 14, 15, 16, 17]. Finally, intermittency can often be found in nonlinear systems that contain an invariant manifold that locally loses its transverse stability properties, e.g., in the motion of finite-size particles in fluids, but also in biological and mechanical systems with slow-fast dynamics [18, 19, 20, 21].

In all of these systems, the complexity of the unstable dynamics is often combined with stochasticity introduced by persistent instabilities that lead to chaotic dynamics as well as by the random characteristics of external excitations. The structure of the stochasticity introduced by these factors plays an important role in the underlying dynamics of the system response. In particular, for a typical case the stochastic excitation is colored noise, i.e., noise with finite correlation time length. Due to the possibility of large excursions by the colored stochastic excitation from its mean value into an "unsafe region," where hidden instabilities are triggered, extreme events may be particularly severe. Therefore, for an accurate description of the probabilistic system dynamics, it is essential to develop analytical methods that will be able to accurately capture the effects of this correlation in the excitation processes for intermittent modes. However, analytical modeling in this case is particularly difficult since, even for low-dimensional systems, standard methods that describe the pdf of the response (such as the Fokker–Planck equation) are not available.

For globally stable dynamical systems numerous techniques have been developed to analyze extreme responses (see, e.g., [22, 23, 24]). There are various steps involved in this case that lead to elegant and useful results, but the starting point is usually the assumption of stationarity in the system response, which is not the case for intermittently unstable systems. Extreme value theory [25, 26, 27, 28, 29] is also a widely applicable method which focuses on thoroughly analyzing the extreme properties of stationary stochastic processes following various distributions. However, even in this case, the analysis does not take into account system dynamics and is usually restricted to very specific forms of correlation functions [25, 26].

Approaches that place more emphasis on the dynamics include averaging of the governing equations. However, the inherently transient character of intermittent instabilities makes it impossible for averaging techniques to capture their effect on the response statistics. Other modeling attempts include approximation of the correlated parametric stochastic excitation by white noise (see, e.g., [30] for an application to parametric ship rolling motion). However, even though this idealization considerably simplifies the analysis and leads to analytical results, it underestimates the intensity of extreme events, since instabilities occur for an infinitesimal amount of time (the process spends an infinitesimal time in the unstable regime, which is

insufficient time for the system to depart from the stable attractor). For this case, heavy-tails can be observed only as long as the parametric excitation is very intense, which for many systems is an unrealistic condition.

In this work, our goal is the development of a method that will allow for the analytical approximation of the probability distribution function (pdf) of modes associated with intermittent instabilities and extreme responses due to parametric excitation by colored noise. This analytic approach will provide a direct link between dynamics and response statistics in the presence of intermittent instabilities. We decompose the problem by conditioning the system response on the occurrence of unstable and stable dynamics through a total probability law argument. This idea enables the separate analysis of the system response in the two regimes and allows us to accurately capture the heavy-tails that arise due to intermittent instabilities. The full probability distribution of the system state is then reconstructed by combining the results from the two regimes. We illustrate this approach on two prototype systems that arise in problems of turbulent flows and nonlinear waves, as well as mechanics. Finally, we thoroughly examine the extent of validity of the derived approximations by direct comparison with Monte Carlo simulations.

2. Problem setup and method. Let $(\Theta, \mathcal{B}, \mathbb{P})$ be a probability space, where Θ is the sample space with $\theta \in \Theta$ denoting an elementary event of the sample space, $\mathcal{B}$ is the associated σ-algebra of the sample space, and $\mathbb{P}$ is a probability measure. We denote by $\mathbb{P}_X$ the probability measure and by p_X the corresponding probability density function, if appropriate, of a random quantity X. In this work we are interested in describing the statistical characteristics of modes subjected to intermittent instabilities. We consider a general dynamical system

$$\dot{\boldsymbol{x}} = G(\boldsymbol{x}, t), \quad \boldsymbol{x} \in \mathbb{R}^n,$$

and assume that its response is an ergodic stochastic process. The presented analysis will rely on the following additional assumptions related to the form of the extreme events:

A1. The instabilities are rare enough that they can be considered statistically independent and have finite duration.

A2. During an extreme event the influenced modes have decoupled dynamics. Moreover, for each one of these modes, during the growth phase, the instability is the governing mechanism; i.e., nonlinear terms are not considered to be important during these fast transitions; they are only considered to be important during the stable dynamics.

A3. After each extreme event there is a relaxation phase that brings the system back to its stable stochastic attractor.

Under these assumptions we may express each intermittent mode, denoted by $u(t;\theta) \in \mathbb{R}$, where $\theta \in \Theta$ (for notational simplicity, we drop explicit dependence on the probability space for random processes whenever clear), as a dynamical system of the form

$$\dot{u} + \alpha(t;\theta)u + \varepsilon\zeta(u, \boldsymbol{v}) = \varepsilon\xi(t;\theta),$$

where $\varepsilon > 0$ is a small quantity and $\zeta(u, \boldsymbol{v})$ is an essentially nonlinear term (nonlinearizable), which may also depend on other system variables $\boldsymbol{v} \in \mathbb{R}^{n-1}$. Since ε is a small quantity, we can assume that the nonlinear term is important only in the stable regime. The stochastic

processes $\alpha(t;\theta)$ and $\xi(t;\theta)$ are assumed stationary with known statistical characteristics. For $\alpha(t)$ we will make the additional assumption that its statistical mean is positive $\overline{\alpha} > 0$ so that the above system has a stable attractor (we denote the mean value operator, the ensemble average, by an overbar $\overline{\square}$). The above equation can be thought of as describing the modulation envelope for a complex mode with a narrow-band spectrum, or one of the coordinates that describe the transverse dynamics to an invariant slow manifold.

The objective of this work is to derive analytical approximations for the pdf of the system response, taking into account intermittent instabilities that arise due to the effect of the stochastic process $\alpha(t)$. In particular, these instabilities are triggered when $\alpha(t) < 0$ and force the system to depart from the stable attractor. Therefore, the system has two regimes where the underlying dynamics behave differently: the stable regime where $\alpha(t) > 0$ and the unstable regime that is triggered when $\alpha(t) < 0$ (Figure 1). Motivated by this behavior, we quantify the system's response by conditioning the probability distribution of the response on stable regimes and unstable events, and we reconstruct the full distribution according to *the law of total probability*,

(1)
$$p_u(x) = p_u(x \mid \text{stable regime})\mathbb{P}(\text{stable regime}) + p_u(x \mid \text{unstable regime})\mathbb{P}(\text{unstable regime}),$$

thereby separating the two regions of interest so that they can be individually studied. The method we employ relies on the derivation of the probability distribution for each of the terms in (1) and then the reconstruction of the full distribution of the system by the total probability law. This idea allows us to capture the dramatically different statistics that govern the system response in the two regimes. Essentially, we decouple the response pdf into two parts: a probability density function with rapidly decaying tails (typically Gaussian) and a heavy-tail distribution with very low probability close to zero. In the following subsections, we provide a description of the method involved for the statistical determination of the terms involved in (1).

2.1. Stochastic description of the stable regime. During the stable regime we have by definition $\alpha > 0$; therefore, under this condition the considered mode is stable. Note that this condition is also true during the relaxation (decay) phase after an extreme event when α switches to positive values $\alpha > 0$ but is not yet relaxed back to the stable attractor. To this end, we cannot directly relate the duration of being on the stable attractor with the probability $\mathbb{P}(\alpha > 0)$, but a correction should be made. We present this correction later in section 2.3. Here we focus on characterizing the probability density function of the system under the assumption that it has relaxed to the stable attractor, and, moreover, we have $\alpha > 0$.

As a first-order estimate of the stable dynamics, we approximate the original dynamical system for the intermittent mode by the stable system

$$\dot{u} + \overline{\alpha}|_{\alpha>0} u + \varepsilon\zeta(u, \boldsymbol{v}) = \varepsilon\xi(t;\theta), \tag{2}$$

where $\overline{\alpha}|_{\alpha>0}$ denotes the conditional average of the process $\alpha(t)$ given that this is positive. The determination of the statistical structure of the stable attractor for (2) can be done with a variety of analytical and numerical methods, such as the Fokker–Planck equation if

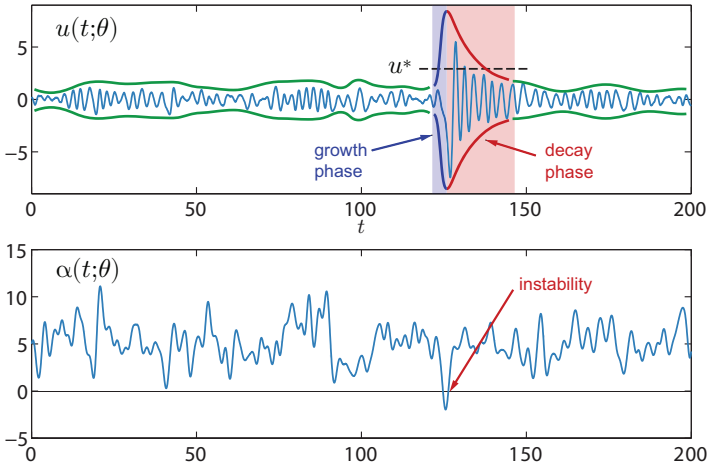

Figure 1. *An intermittently unstable system. The system (top) experiences a large magnitude response when the parametric excitation process (bottom) crosses the zero level. Dashed green lines denote the envelope of the process during the stable regime. The transient instability can be described by two stages, an exponential growth phase and then a subsequent decay phase that relaxes the response back to the stable regime.*

the process $\xi(t)$ is white noise (see, e.g., [31, 23]) or the joint response-excitation equations otherwise [32, 33]. Using one of these methods, we can obtain the pdf for the statistical steady state of the system $\mathbb{P}(u \mid \text{stable regime})$.

2.2. Stochastic description of the growth phase. In contrast to the stable regime, the unstable regime is far more complicated due to its inherently transient nature. In addition, the unstable regime consists of two distinct phases: a growth phase where $\alpha < 0$, with positive system Lyapunov exponent, and a subsequent decay phase that starts when α has a zero upcrossing and is characterized by $\alpha > 0$, with negative system Lyapunov exponent. We first consider the growth phase, where we rely on assumption A2, according to which the dominant mechanism is the term related to the instability. Under this assumption, the first-order approximation during the growth phase is governed by the system

$$\dot{u} + \alpha(t;\theta)u = 0 \implies u(t;\theta) = u_0 e^{\Lambda T},$$

where u_0 is a random initial condition described by the probability measure in the stable regime, T is the random duration of the downcrossing event $\alpha < 0$, and Λ is the growth exponent, which, for each extreme event with t^* representing the time of the start of the instability, can be approximated by

$$\Lambda \simeq -\frac{1}{T}\int_{t^*}^{t^*+T} \alpha(t;\theta)\, dt,$$

due to the rapid nature of the growth phase. Therefore, during the growth phase we have

$$\mathbb{P}(u > u^* \mid \alpha < 0) = \mathbb{P}(u_0 e^{\Lambda T} > u^* \mid \alpha < 0) = \mathbb{P}(u_0 e^{\Lambda T} > u^* \mid \alpha < 0, u_0)\mathbb{P}(u_0), \tag{3}$$

where u^* represents the value of the response that we are interested in. The right-hand side of (3) is a derived distribution depending on the probabilistic structure of Λ and T.

The initial value u_0 is a random variable with statistical characteristics corresponding to the stable regime of the system, in other words by $\mathbb{P}(u \mid \text{stable regime})$. Hence, to determine the required probability distribution we need only to know $\mathbb{P}(\alpha, T \mid \alpha < 0)$, i.e., the joint pdf of α (given that this is negative) and the duration of the time interval over which α is negative. This distribution involves only the excitation process α, and for the Gaussian case it can be approximated analytically (see section 3). Alternatively, one can compute this distribution using numerically generated random realizations that respect the statistical characteristics of the process.

2.3. Stochastic description of the decay phase. The decay phase is also an inherently transient stage. It occurs right after the growth phase of an instability, when α has an upcrossing of the zero level, and is therefore characterized by positive values of α, with the effect of driving the system back to the stable attractor. To provide a statistical description of the relaxation phase, we first note the strong connection between the growth and decay phases. In particular, as shown in Figure 1, for each extreme event there is a one-to-one correspondence for the values of the intermittent variable u between the growth phase and the decay phase. By focusing on an individual extreme event, we note that the probability of u exceeding a certain threshold during the growth phase is equal with the probability of u exceeding the same threshold during the decay phase. Thus over the total instability we have

$$\begin{aligned}&\mathbb{P}(u > u^* \mid \text{unstable regime})\\ &\quad = \mathbb{P}(u > u^* \mid \text{instability} - \text{decay}) = \mathbb{P}(u > u^* \mid \text{instability} - \text{growth}),\end{aligned}$$

where the conditional distribution for the growth phase has been determined in (3).

2.4. Probability of the stable and the unstable regimes. In the final step we determine the relative duration of the stable and unstable regimes. To do so, we rely on the ergodic property of the response process. This allows us to quantify the probability of a stable and an unstable event in terms of their temporal durations. The probability of having an instability is simply $\mathbb{P}(\alpha < 0)$; however, due to the decay phase the duration of an instability will be longer than the duration of the event $\alpha < 0$. To determine the typical duration of the decay phase, we first note that during the growth phase we have

$$u_p = u_0 e^{-\overline{\alpha}|_{\alpha<0} T_{\alpha<0}}, \tag{4}$$

where $T_{\alpha<0}$ is the duration for which $\alpha < 0$ and u_p is the peak value of u during the instability. Similarly, for the decay phase we utilize system (2) and obtain

$$u_0 = u_p e^{-\overline{\alpha}|_{\alpha>0} T_{\text{decay}}}. \tag{5}$$

Combining the last two equations (4) and (5), we have

$$\frac{T_{\alpha<0}}{T_{\text{decay}}} = -\frac{\overline{\alpha}|_{\alpha>0}}{\overline{\alpha}|_{\alpha<0}}. \tag{6}$$

This equation (6) expresses the typical ratio between the growth and the decay phases. Thus, the total duration of an unstable event is given by the sum of the duration of these two phases

$$T_{\text{inst}} = \left(1 - \frac{\overline{\alpha}|_{\alpha<0}}{\overline{\alpha}|_{\alpha>0}}\right) T_{\alpha<0}. \tag{7}$$

Using this result, we can express the total probability of being in an unstable regime by

$$\mathbb{P}(\text{unstable regime}) = \left(1 - \frac{\overline{\alpha}|_{\alpha<0}}{\overline{\alpha}|_{\alpha>0}}\right)\mathbb{P}(\alpha < 0).$$

Note that since we have assumed in A1 that instabilities are sufficiently rare that instabilities do not overlap and that instabilities are statistically independent, we will always have $\mathbb{P}(\text{unstable regime}) < 1$. Hence, the corresponding probability of being in the stable regime is

$$\mathbb{P}(\text{stable regime}) = 1 - \left(1 - \frac{\overline{\alpha}|_{\alpha<0}}{\overline{\alpha}|_{\alpha>0}}\right)\mathbb{P}(\alpha < 0).$$

3. Instabilities driven by Gaussian processes. In this section, we recall relevant statistical properties associated with a Gaussian stochastic parametric excitation. The zero level of the stochastic process $\alpha(t)$ defines the boundary between a stable and an unstable response. Therefore, the statistics that are relevant include the probability that the stochastic process is above and below the zero level, the average duration spent below and above the zero level, and the probability distribution of the length of time intervals spent below the zero level.

For convenience, let $\alpha(t;\theta) = m + k\gamma(t;\theta)$, where $\gamma(t)$ is also an ergodic and stationary Gaussian process, but with zero mean and unit variance, so that $\alpha(t)$ has mean m and variance k^2. Thus the threshold of a rare event in terms of $\gamma(t)$ is given by the parameter $\eta \equiv -m/k$. We assume that second order properties, such as the power spectrum, of $\gamma(t)$ are known. In such a case, the correlation of the process is given by

$$R_\gamma(\tau) = \int_{-\infty}^{\infty} S_\gamma(\omega) e^{i\omega\tau}\, d\omega.$$

In addition, we denote by $\phi(\,\cdot\,)$ the standard normal probability density function and by $\Phi(\,\cdot\,)$ the standard normal cumulative probability density function. Since $\gamma(t)$ is a stationary Gaussian process, the probability that the stochastic process is in the two states $\mathbb{P}(\alpha < 0)$ and $\mathbb{P}(\alpha > 0)$ is, respectively, $\mathbb{P}(\gamma < \eta) = \Phi(\eta)$ and $\mathbb{P}(\gamma > \eta) = 1 - \Phi(\eta)$.

3.1. Average time below and above the zero level. Here we determine the average length of the intervals that $\alpha(t)$ spends above and below the zero level. For the case $\alpha(t) < 0$, that is, $\gamma(t) < \eta$, the expected number of upcrossings of this threshold per unit time is given by Rice's formula [34, 35] (for a stochastic process with unit variance)

$$\overline{N^+}(\eta) = \int_0^\infty u p_{\gamma\dot{\gamma}}(\eta, u)\, du = \frac{1}{2\pi}\sqrt{-R_\gamma''(0)}\exp(-\eta^2/2), \tag{8}$$

where $\overline{N^+}(\eta)$ is the average number of upcrossings of level η per unit time, which is equivalent to the average number of downcrossings $\overline{N^-}(\eta)$, and $p_{\gamma\dot{\gamma}}$ is the joint pdf of γ and its time derivative $\dot{\gamma}$. The expected number of crossings is finite if and only if $\gamma(t)$ has a finite second spectral moment [35].

The average length of the interval that $\gamma(t)$ spends below the threshold η can then be determined by noting that this probability is given by the product of the number of downcrossings of the threshold per unit time and the average length of the intervals for which $\gamma(t)$

is below the threshold η [36]

$$\overline{T}_{\alpha<0} = \frac{\mathbb{P}(\gamma < \eta)}{\overline{N^-}(\eta)}.$$

Hence, using the result (8), we have

$$\overline{T}_{\alpha<0}(\eta) = \frac{2\pi \exp(\eta^2/2)}{\sqrt{-R''_\gamma(0)}}\Phi(\eta). \tag{9}$$

3.2. Distribution of time below the zero level. Here we recall a result regarding the distribution of time that the stochastic process $\gamma(t)$ spends below the threshold level η, i.e., the probability of the length of intervals for which $\gamma(t) < \eta$.

In general, it is not possible to derive an exact analytical expression for the distribution of time intervals given $\gamma(t) < \eta$—in other words the distribution of the length of time between a downcrossing and an upcrossing. However, the asymptotic expression in the limit $\eta \to -\infty$ is given by [36] (henceforth we denote $\overline{T}_{\alpha<0}$ by $\overline{T}$ for simplicity)

$$p_T(t) = \frac{\pi t}{2\overline{T}^2} \exp\bigl(-\pi t^2/4\overline{T}^2\bigr), \tag{10}$$

which is a Rayleigh distribution with scale parameter $\sqrt{2\overline{T}^2/\pi}$, where $\overline{T}$ is given by (9). This approximation is valid for small interval lengths t, since the derivation assumes that when a downcrossing occurs at time t_1 only a single upcrossing occurs at time $t_2 = t_1 + t$, neglecting the possibility of multiple crossings in between the two time instances. In Figure 2 the analytic distribution (10) is compared with numerical results, and, as expected, we see that the analytic expression agrees well with the numerical results for small interval lengths, where the likelihood of multiple upcrossings in the interval is small. In addition, note that the only relevant parameter of the stochastic process $\gamma(t)$ that controls the scale of the distribution in (10) is the mean time spent below the threshold level, which depends only on the threshold η and $R''_\gamma(0)$.

4. Application to a parametrically excited mechanical oscillator. Having formulated the general method, we proceed to the first application, to that of a parametrically excited mechanical oscillator. Specifically, we consider the following single-degree-of-freedom oscillator under parametric stochastic excitation and additive white noise forcing:

$$\ddot{x}(t) + c\dot{x}(t) + \kappa(t;\theta)x(t) = \sigma_x \dot{W}(t;\theta), \tag{11}$$

where c and σ_x are constants, $\kappa(t;\theta)$ is a stationary and ergodic Gaussian process of a given power spectrum $S_\kappa(\omega)$ with mean m and variance k^2, and $\dot{W}(t;\theta)$ is white noise. As before, $\eta \equiv -m/k$ defines the extreme event threshold. We may write (11) in the state space form

$$\begin{aligned} dx_1 &= x_2\, dt, \\ dx_2 &= -\bigl(cx_2 + \kappa(t)x_1\bigr)\, dt + \sigma_x\, dW(t). \end{aligned} \tag{12}$$

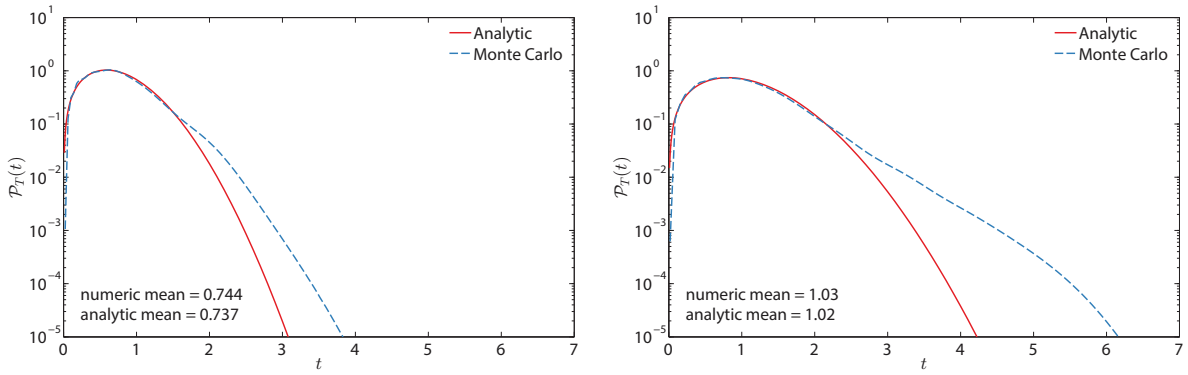

Figure 2. *Comparison of the analytic distribution $p_T(t)$ (10) with Monte Carlo simulation, generated using 1000 ensembles of a Gaussian process with correlation $R(\tau) = \exp(-\tau^2/2)$ from $t_0 = 0$ to $t_f = 1000$, for two different sets of parameters: $m = 5.0$, $k = 1.6$ (left); $m = 5.0$, $k = 2.4$ (right).*

Our presentation will follow section 2, although the analytical expressions for the pdf will be computed directly for position and velocity (instead of the envelope process u as done in section 2) for instructive purposes. At the end of this section we present comparisons with direct numerical simulations and thoroughly examine the limits of validity for the approximations we have made.

4.1. Probability distribution in the stable regime. We first derive the probability distribution for the system under consideration given that the system is in the stable regime. Following section 2.1, we replace $\kappa(t)$ by the mean $\omega_s^2 = \overline{\kappa}|_{\kappa>0}$. This approximation is valid since only small fluctuations of the process $\kappa(t)$ around the mean ω_s^2 occur in this state, and these fluctuations have a minor impact on the system's probabilistic response.

Making this approximation, (12) becomes

$$\ddot{x}(t) + c\dot{x}(t) + \omega_s^2 x(t) = \sigma_x \dot{W}(t).$$

To determine the mean ω_s^2, note that its pdf is given by $p_\kappa(x \mid \kappa > 0) = \phi((x-m)/k)/(k(1-\Phi(\eta)))$; hence

$$\omega_s^2 = \overline{\kappa}|_{\kappa>0} = m + k\frac{\phi(\eta)}{1-\Phi(\eta)}. \tag{13}$$

The density in the stable regime can now be found by seeking a stationary solution of the Fokker–Planck equation of the form $p(x_1, x_2) = p(H)$, where $H = \frac{1}{2}(\omega_s^2 x_1^2 + x_2^2)$ is the total mechanical energy of the system. In this case the Fokker–Planck equation simplifies to [23]

$$cp(H) + \frac{1}{2}\sigma_x^2 \frac{dp}{dH} = 0 \implies p(H) = q\exp\left(-\frac{2c}{\sigma_x^2}H\right),$$

where $q = c\omega_s/(\pi\sigma_x^2)$ is a normalization constant. Taking the marginal with respect to x_2 gives the probability density for the system's position,

$$p_{x_1}(x \mid \kappa > 0) = \sqrt{\frac{c\omega_s^2}{\pi\sigma_x^2}}\exp\left(-\frac{c\omega_s^2}{\sigma_x^2}x^2\right), \tag{14}$$

which is Gaussian with variance $\sigma^2 = \sigma_x^2/(2c\omega_s^2)$. Similarly, taking the marginal with respect to x_1 gives the probability density for the system's velocity,

$$p_{x_2}(x \mid \kappa > 0) = \sqrt{\frac{c}{\pi\sigma_x^2}} \exp\left(-\frac{c}{\sigma_x^2}x^2\right), \tag{15}$$

where the variance is $\sigma^2 = \sigma_x^2/(2c)$.

4.2. Probability distribution in the unstable regime. Here we derive the probability distribution for the system's position x_1 during the growth stage of an instability. In the unstable regime, the system initially undergoes exponential growth due to the stochastic process $\kappa(t)$ crossing below the zero level, which is the mechanism that triggers the instability. After a finite duration of exponential growth, which stops when $\kappa(t)$ crosses above the zero level, and due to the large velocity gradients that result, friction damps the response back to the stable attractor. Following assumption A2, we consider the parametric excitation as the primary mechanism driving the instability during the growth phase and therefore ignore the effect of friction during this stage of the instability.

We treat the system response as a narrow-band process. This means that the response has a spectrum that is narrowly distributed around a mean frequency, i.e., $q = \sigma_s/\omega_s \ll 1$, where $\omega_s = \int \omega S(\omega)\, d\omega$ and $\sigma_s^2 = \int (\omega - \omega_s)^2 S(\omega)\, d\omega$ [37]. We can therefore describe the instability in terms of the envelope u for the position variable by averaging over the fast frequency ω_s. During the growth phase we have $u \simeq u_0 \exp(\Lambda T)$, where u_0 is the random value of the position's envelope before an instability (to be determined in section 4.3), T is the random duration of the event $\kappa < 0$, and Λ is the random growth exponent, which will be the same for both the position and the velocity variables. Substituting this representation into (11), we find $\Lambda^2 + \kappa \simeq 0$, so that the positive eigenvalue is given by $\Lambda \simeq \sqrt{-\kappa}$. To proceed, we set $u = u_0 \exp(\Lambda T)$ and $y = \Lambda$; then, from a change of variables,

$$p_{uy}(u, y) = p_{\Lambda T}(\lambda, t) |\det[\partial(\lambda, t)/\partial(u, y)]|,$$

where we understand that the pdf is conditional upon $\kappa < 0$ and a fixed u_0. Next we assume that T and Λ are independent (see Figure 3). Then, we have

$$p_{uy}(u, y) = \frac{p_\Lambda(\lambda) p_T(t)}{u_0 \lambda \exp(\lambda t)} = \frac{1}{uy} p_\Lambda(y) p_T\left(\frac{\log(u/u_0)}{y}\right), \quad u > u_0,\ y > 0.$$

Taking the marginal density gives

$$p_u(u) = \frac{1}{u} \int_0^\infty \frac{1}{y} p_\Lambda(y) p_T\left(\frac{\log(u/u_0)}{y}\right) dy. \tag{16}$$

Now, since $\mathbb{P}(\Lambda) = \mathbb{P}(\sqrt{-\kappa} | \kappa < 0)$, from another change of variables we obtain

$$p_\Lambda(\lambda) = \frac{2\lambda}{\Phi(\eta)} p_\kappa(-\lambda^2) = \frac{2\lambda}{k\Phi(\eta)} \phi\left(-\frac{\lambda^2 + m}{k}\right), \quad \lambda > 0,$$

since $\mathbb{P}(\kappa)$ is normally distributed. Combining this result and the fact that p_T is given by the Rayleigh distribution (10) with (16) gives the final result for the probability density function, (17)

$$p_u(u \mid \kappa < 0, u_0) = \frac{\pi \log(u/u_0)}{k\overline{T}^2 \Phi(\eta) u} \int_0^\infty \frac{1}{y} \phi\left(-\frac{y^2+m}{k}\right) \exp\left(-\frac{\pi}{4\overline{T}^2 y^2} \log(u/u_0)^2\right) dy, \quad u > u_0,$$

where $\overline{T}$ denotes the conditional average $\overline{T}_{\kappa<0}$. Moreover, utilizing the expression for the duration of a typical extreme event (7), we obtain for this particular system

$$T_{\text{inst}} = \left(1 + \frac{2\overline{\Lambda}_{\kappa<0}}{c}\right) T_{\kappa<0}, \tag{18}$$

where for the relaxation phase we have the rate of decay for the envelope being $-c/2$.

To formulate our result in terms of the position variable, we refer to the narrow-band approximation made at the beginning of this analysis. This will give approximately $x_1 = u\cos\varphi$, where φ is a uniform random variable distributed between 0 and 2π. The probability density function for $z = \cos\varphi$ is given by $p_z(x) = 1/(\pi\sqrt{1-x^2})$, $x \in [-1, 1]$. To avoid double integrals for the computation of the pdf for the position, we approximate the pdf for z by $p_z(x) = \frac{1}{2}(\delta(x+1) + \delta(x-1))$. This will give the following approximation for the conditionally unstable pdf:

$$p_{x_1}(x \mid \kappa < 0, u_0) = \frac{1}{2} p_u(|x| \mid \kappa < 0, u_0). \tag{19}$$

We note that, as presented in section 2, the pdf for the envelope u may also be used for the decay phase. However, during the decay phase the oscillatory character (with frequency ω_s) of the response has to also be taken into account. Nevertheless, to keep the expressions simple we will use (19) to describe the pdf for the position in the decay phase as well. We will show in the following sections that this approximation compares favorably with numerical simulations.

4.2.1. Integral approximation for the conditionally unstable pdf. We derive an asymptotic expansion, as $u \to \infty$, for the integral (17) that describes the distribution for the position's envelope during the growth phase of an instability, treating u_0 as a parameter. For convenience in (17) let $p_u(u \mid \kappa < 0, u_0) = \int_0^\infty \xi(u, y; u_0)\, dy$, that is,

$$\begin{aligned}\xi(u, y; u_0) &= \frac{\pi \log(u/u_0)}{\sqrt{2\pi} k\overline{T}^2 \Phi(\eta) u y} \exp\left(-\frac{(y^2+m)^2}{2k^2} - \frac{\pi}{4\overline{T}^2 y^2} \log(u/u_0)^2\right) \\ &= \frac{\pi \log(u/u_0)}{\sqrt{2\pi} k\overline{T}^2 \Phi(\eta) u y} \exp(\theta(u, y; u_0)),\end{aligned}$$

where $\theta(u, y; u_0)$ denotes the terms being exponentiated (we suppress the explicit dependence on the parameter u_0 for convenience); in other words,

$$p_u(u \mid \kappa < 0, u_0) = \int_0^\infty \xi(u, y; u_0)\, dy = \frac{\pi \log(u/u_0)}{\sqrt{2\pi} k\overline{T}^2 \Phi(\eta) u} \int_0^\infty \frac{1}{y} \exp(\theta(u, y))\, dy.$$

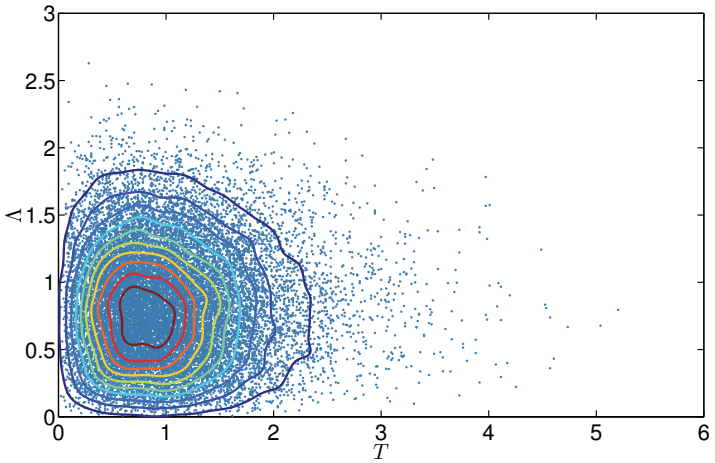

Figure 3. *Scatter plot and contours of the joint pdf of T and Λ for $\eta = -2.08$ ($m = 5.00$, $k = 2.40$). Samples for Λ are drawn by inverse-sampling the cumulative distribution function, and samples of T are drawn from realizations of a Gaussian process using 1000 ensembles of time length $t = 1000$.*

This integral can be approximated following Laplace's method, where in this case we have a moving maximum [38]. For fixed u the exponential is distributed around its peak value $y^* = \max_y \exp(\theta(u, y; u_0))$, so that we may make the following approximations to leading order:

$$\begin{aligned} p_u(u \mid \kappa < 0, u_0) &\simeq \frac{\pi \log(u/u_0)}{\sqrt{2\pi} k \overline{T}^2 \Phi(\eta) u} \int_{y^*-\epsilon}^{y^*+\epsilon} \frac{1}{y^*} \exp\left(\theta(u, y^*) + \frac{(y-y^*)^2}{2} \partial_{yy}\theta(u, y^*) + \cdots \right) dy \\ &\simeq \xi(u, y^*; u_0) \int_{-\infty}^{\infty} \exp\left(\frac{(y-y^*)^2}{2} \partial_{yy}\theta(u, y^*) + \cdots \right) dy \\ &= \frac{1}{\tilde{c}} \xi(u, y^*; u_0), \end{aligned}$$

where $\tilde{c}$ is a normalization constant that is computed numerically. In order to arrive at a closed analytic expression for $y^* = \max_y \exp(\theta(u, y))$, we find that the following expression is a good approximation for y^* (see the appendix for details):

$$y^*(u; u_0) = \left(\frac{\pi k^2}{4m\overline{T}^2} \right)^{1/4} \log(u/u_0)^{1/2}, \quad m^2 \gg k^2.$$

Hence, we have the following expression that approximates the original integral:

$$p_u(u \mid \kappa < 0, u_0) \simeq \frac{1}{\tilde{c}} \xi(u, y^*; u_0), \quad m^2 \gg k^2. \tag{20}$$

In our case the assumption is that instabilities are sufficiently rare that the standard deviation k of the Gaussian process $\kappa(t)$ will be smaller than its mean m, and the condition $m^2 \gg k^2$ in (20) will be approximately satisfied. Indeed, the derived asymptotic expansion (20) and the exact integral (17) show excellent agreement, even for small values of u (see Figure 4).

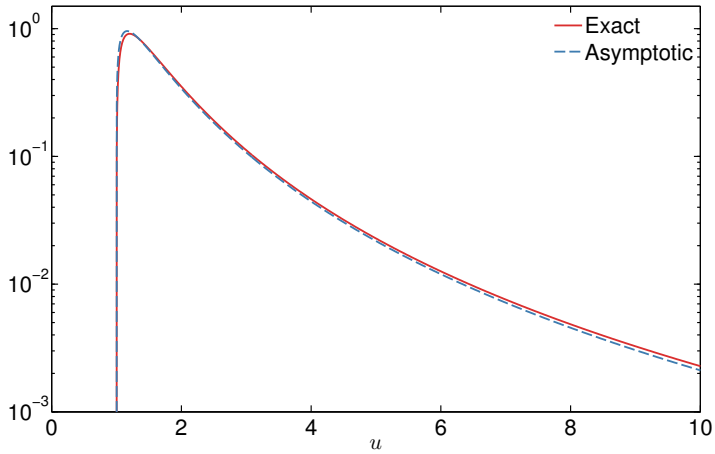

Figure 4. *Exact integral in* (17) *compared to the asymptotic expansion given in* (20) *for a fixed* u_0 *and* $m = 5.00$, $k = 2.00$.

4.3. Probability density function for the envelope in the stable regime. In the derivation of the probability density in the unstable regime we conditioned the result on the initial value of the position's envelope right before an instability occurs. The stable regime's envelope is defined as the locus of local maxima of the stationary Gaussian process that governs the system before an instability. For a stationary Gaussian process of zero mean the joint probability density of the envelope and the envelope velocity is given by [39]

$$p(u,\dot{u}) = \frac{u}{q\lambda_0\sqrt{2\pi\lambda_2}} \exp\left\{-\frac{1}{2}\left(\frac{u^2}{\lambda_0} + \frac{\dot{u}^2}{q^2\lambda_2}\right)\right\}, \tag{21}$$

where λ_n is the nth order spectral moment for the one-sided power spectral density of x_1 in the stable regime and $q^2 = 1 - \lambda_1^2/\lambda_0\lambda_2$ describes the extent to which the process is narrow-banded. In our case, we are interested in the pdf of the envelope for the position $\mathbb{P}(u_0)$; marginalizing out $\dot{u}$ from (21) gives

$$p(u) = \int_{-\infty}^{\infty} p(u,\dot{u})\, d\dot{u} = \frac{u}{\lambda_0} \exp(-u^2/2\lambda_0), \tag{22}$$

which is a Rayleigh distribution with scale parameter $\sqrt{\lambda_0}$. The zeroth-order spectral moment is the variance of the Gaussian pdf in (14), i.e., $\lambda_0 = \sigma_x^2/(2c\omega_s^2)$, and thus

$$p_{u_0}(x) = \frac{2c\omega_s^2 x}{\sigma_x^2} \exp(-c\omega_s^2 x^2/\sigma_x^2).$$

The pdf above determines the distribution of the initial point of the instability u_0. We use this result to marginalize out u_0 from the pdf of the unstable distribution derived in section 4.2, which was conditioned on a fixed initial point of an instability. Using (19) and (20) this gives

the final result for the density in the unstable regime:

$$p_{x_1}(x \mid \kappa < 0) = \frac{1}{2}\int p_u(|x| \mid \kappa < 0, u_0) p_{u_0}(u_0)\, du_0$$

$$= \frac{1}{2\tilde{c}}\int_0^{|x|} \xi(|x|, y^*(|x|; u_0); u_0) p_{u_0}(u_0)\, du_0. \tag{23}$$

4.4. Probability density function for the velocity. The probability density for the system's velocity x_2 in the stable regime can be found by marginalizing the solution obtained from the Fokker–Planck equation (15). The same result may be obtained by relying on the narrow-band property of the stochastic response in the stable regime. In particular, we may represent the stochastic process for position x_1 in terms of its spectral power density [24]:

$$x_1 = \int_0^\infty \cos(\omega t + \varphi(\omega))\sqrt{2S_x(\omega)\, d\omega},$$

where the last integral is defined in the mean square sense. Differentiating the above, we obtain

$$x_2 = \int_0^\infty \omega \cos\Big(\omega t + \varphi(\omega) + \frac{\pi}{2}\Big)\sqrt{2S_x(\omega)\, d\omega}$$

$$\simeq \omega_s \int_0^\infty \cos\Big(\omega t + \varphi(\omega) + \frac{\pi}{2}\Big)\sqrt{2S_x(\omega)\, d\omega},$$

using the narrow-band property of the spectral density around ω_s. Note that the integral in the last equation has the same distribution as x_1. Thus, it is easy to prove that the probability density function of x_2 in the *stable regime* is given by the pdf of $\omega_s x_1$.

In the unstable regime stationarity breaks down, and the envelope of the stochastic processes describing position changes with time. This has an important influence on the probabilistic structure for the velocity, which cannot be approximated as was done in the stable regime. The reason is that we have an additional time scale associated with the variation of the envelope of the narrow-band oscillation (see Figure 5). For the purpose of computing the pdf for velocity in the unstable regime, we approximate the envelope for position during the instability by a sine function with a half-period equal to the average duration of the extreme events (equation (18)) $T_{\text{inst}} = (1 + 2\overline{\Lambda}_{\kappa<0}/c)T_{\kappa<0}$. This gives the following approximate expression for the unstable regime:

$$x_1 = \left(1 + \frac{u_p}{u_0}\right)\sin(\omega_u t)\int_0^\infty \cos(\omega t + \varphi(\omega))\sqrt{2S_x(\omega)\, d\omega},$$

where u_p/u_0 is the ratio of the extreme event peak value for the envelope over the initial value of the envelope (before the extreme event), and $\omega_u = \pi/T_{\text{inst}}$. Assuming that $u_p/u_0 \gg 1$, we have that the pdf for velocity during the *unstable regime* is also given in terms of x_1 but with the different scaling factor

$$x_2 \sim \frac{1}{2}\left(\omega_s + \frac{\pi}{(1 + 2\overline{\Lambda}_{\kappa<0}/c)\overline{T}}\right)x_1.$$

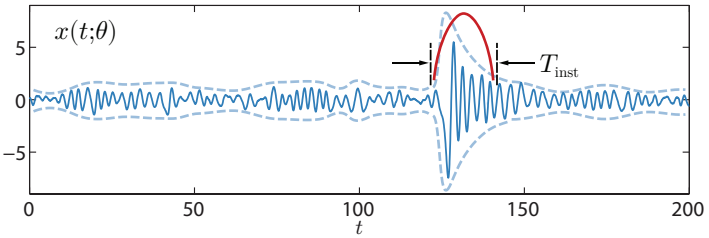

Figure 5. *For the computation of the velocity pdf, we approximate the envelope of the process during the extreme event with a harmonic function of consistent period.*

The last relation gives a direct expression for the pdf of velocity in the unstable regime. Using this scaling factor $\omega_{\text{inst}} = (\omega_s + \omega_u)/2$ for the conditionally unstable pdf and the correct scaling for the stable regime ω_s, we can derive an approximation for the pdf of velocity (given in section 4.5).

4.5. Summary of results for the parametrically excited oscillator.

Probability distribution function for the position. Combining the results of (14), (23), and (18) according to the law of total probability (1) gives the following heavy-tailed, symmetric probability density function for the position:

$$p_{x_1}(x) = \big(1 - (1 + 2\overline{\Lambda}_{\kappa<0}/c)\Phi(\eta)\big)\sqrt{\frac{c\omega_s^2}{\pi\sigma_x^2}}\exp\left(-\frac{c\omega_s^2}{\sigma_x^2}x^2\right) + (1 + 2\overline{\Lambda}_{\kappa<0}/c)\Phi(\eta)\int_0^{|x|}\frac{1}{2\tilde{c}}\xi(|x|, y^*(|x|;x_0);x_0)p_{u_0}(x_0)\,dx_0, \quad x \in \mathbb{R}. \tag{24}$$

Writing each term explicitly, we have

$$p_{x_1}(x) = \big(1 - (1 + 2\overline{\Lambda}_{\kappa<0}/c)\Phi(\eta)\big)\sqrt{\frac{c\omega_s^2}{\pi\sigma_x^2}}\exp\left(-\frac{c\omega_s^2}{\sigma_x^2}x^2\right) + (1 + 2\overline{\Lambda}_{\kappa<0}/c)\Phi(\eta)$$
$$\cdot\frac{\sqrt{2\pi}cw_s^2}{2\tilde{c}\sigma_x^2 k\overline{T}^2\Phi(\eta)}\int_0^{|x|}\frac{\log(|x|/x_0)}{(|x|/x_0)y^*(|x|;x_0)}\exp\left(-\frac{(y^*(|x|;x_0)^2 + m)^2}{2k^2} - \frac{\pi\log(|x|/x_0)^2}{4\overline{T}^2 y^*(|x|;x_0)^2} - \frac{c\omega_s^2}{\sigma_x^2}x_0^2\right)dx_0.$$

Probability distribution function for the velocity. To obtain the pdf for velocity we scale the pdf for the position in (24). As noted in section 4.4, the correct scaling for the first term in (1), which represents the stable regime, is given by ω_s, and for the second term, for the unstable regime, the scaling is given by ω_{inst}. Applying the random variable transformation $p_{x_2}(x) = p_{x_1}(x/\omega)/\omega$ with the appropriate scaling for each of these two terms yields

$$p_{x_2}(x) = \big(1 - (1 + 2\overline{\Lambda}_{\kappa<0}/c)\Phi(\eta)\big)\sqrt{\frac{c}{\pi\sigma_x^2}}\exp\left(-\frac{c}{\sigma_x^2}x^2\right) + (1 + 2\overline{\Lambda}_{\kappa<0}/c)\Phi(\eta)\int_0^{|x|/\omega_{\text{inst}}}\frac{1}{2\omega_{\text{inst}}\tilde{c}}\xi(|x|/\omega_{\text{inst}}, y^*(|x|/\omega_{\text{inst}};x_0');x_0')p_{u_0}(x_0')\,dx_0', \quad x \in \mathbb{R}. \tag{25}$$

For the integral in the second term in (25), making the substitution $x_0 = \omega_{\text{inst}} x_0'$, we have

$$p_{x_2}(x \mid \kappa < 0) = \frac{\sqrt{2\pi}c}{2\tilde{c}\sigma_x^2 k\overline{T}^2\Phi(\eta)} \frac{\omega_s^2}{\omega_{\text{inst}}^2} \int_0^{|x|} \frac{\log(|x|/x_0)}{(|x|/x_0)y^*(|x|;x_0)} \cdot \exp\left(-\frac{(y^*(|x|;x_0)^2+m)^2}{2k^2} - \frac{\pi \log(|x|/x_0)^2}{4\overline{T}^2 y^*(|x|;x_0)^2} - \frac{c}{\sigma_x^2}\frac{\omega_s^2}{\omega_{\text{inst}}^2}x_0^2\right) dx_0. \tag{26}$$

Therefore, rewriting (25) gives the following pdf for velocity:

$$p_{x_2}(x) = \left(1 - (1 + 2\overline{\Lambda}_{\kappa<0}/c)\Phi(\eta)\right)\sqrt{\frac{c}{\pi\sigma_x^2}}\exp\left(-\frac{c}{\sigma_x^2}x^2\right) + (1 + 2\overline{\Lambda}_{\kappa<0}/c)\Phi(\eta)\int_0^{|x|} \frac{1}{2\omega_{\text{inst}}\tilde{c}}\xi(|x|, y^*(|x|;x_0);x_0)p_{u_0}(x_0/\omega_{\text{inst}})\,dx_0, \tag{27}$$

where the integral in the second term is explicitly given in (26).

4.6. Comparison with direct Monte Carlo simulations and range of validity. Here we discuss the analytic results for the system response pdf given in section 4.5, present comparisons with Monte Carlo simulations, and describe the effect of varying system parameters on the analytical approximations. In addition, we examine the region of validity of our results with respect to these parameters.

First, in Figure 6 a sample system response is shown alongside the corresponding signal of the parametric excitation. This sample realization is characteristic of the typical system response for the case under study (rare instabilities of finite duration). During the brief period when $\kappa(t) < 0$, at approximately $t = 85$, the system experiences exponential growth, and when the parametric excitation process $\kappa(t)$ returns above the zero level, friction damps the system response from growing indefinitely, returning the system to the stable state after a short decay phase.

In Figure 7, a typical decomposition of the stable and unstable parts of the full response pdf is presented. We emphasize that the tails in the system response pdf are completely described by the term in the total probability law that accounts for system instabilities, whereas the inner core of the pdf is mainly due to the term in the total probability decomposition that corresponds to the solution in the stable regime. Despite the fact that the system spends practically all of its time in a stable state, the stable part in the expression for the response pdf contributes essentially nothing to the tails of the distribution. The tails, in other words, completely describe the statistics of system instabilities, which are highly non-Gaussian and are described by a fat-tailed distribution.

The analytical results for the system response pdf given in (24) and (27) have been derived under a careful set of assumptions. We observe that if the frequency of instabilities is large or if damping is weak (i.e., extreme events of long duration), or if there is any parameter combination such that the conditionally unstable pdf in the total probability decomposition (1) contributes significantly to the stable state, then our analytical results will likely overestimate the probability near the Gaussian core and underestimate the tail probabilities. This behavior is expected, since our assumptions are no longer strictly valid. If this is the case, a cusp near

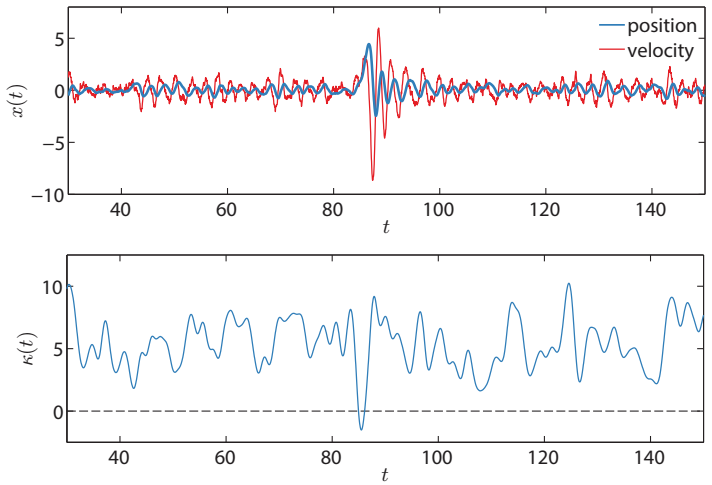

Figure 6. *Sample realization (top) and the corresponding parametric excitation process (bottom) demonstrating the typical system response during an intermittent event for position (in thick blue) and velocity (in thin red) for* $\eta = -2.27$ *(*$k = 2.2$*,* $m = 5.0$*),* $c = 0.53$*.*

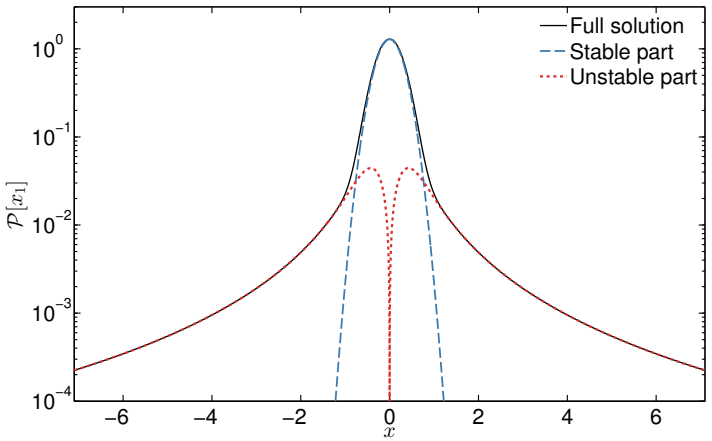

Figure 7. *Typical superposition of the stable (in dashed blue) and unstable (in dotted red) part of the total probability law decomposition* (1) *of the full analytical pdf.*

the mean state may be observed in our analytical expressions for the pdf, which is due to the approximation made in section 4.2, where we approximate the conditionally unstable pdf for the position variable in terms of its envelope (19) (see Figure 8). This phenomenon is more pronounced in the pdf for the velocity x_2, since the unstable part of the decomposition (1) is scaled by a frequency that is smaller than the stable part, which pushes more probability toward the Gaussian core. A minor contributing factor to the severity of this cusp is due to the integral asymptotic expansion made in section 4.2.1; the asymptotic expression in (20) displays sharper curvature near u_0, when compared to the exact integral in (20), resulting in a slightly more pronounced cusp.

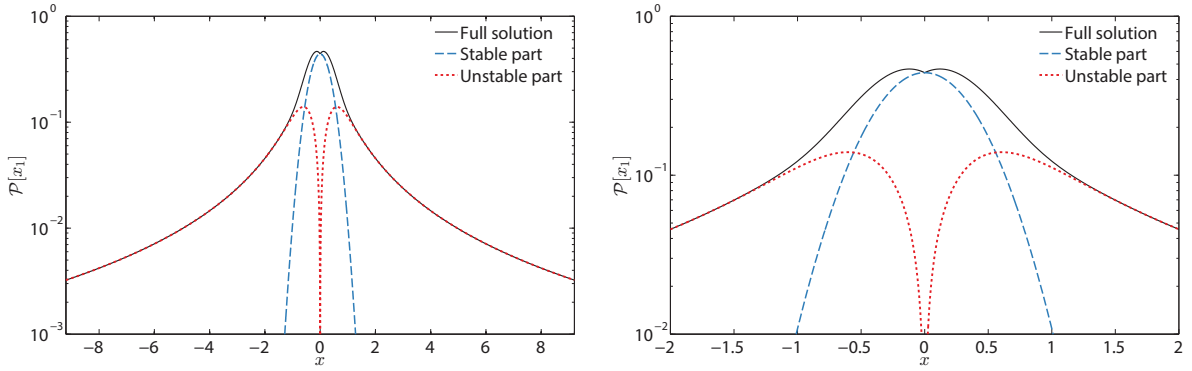

Figure 8. *Demonstration of the cusp phenomenon, which is prominent in regimes with very frequent instabilities and/or instabilities of long duration, due to approximations made in the unstable regime.*

4.6.1. Comparison with Monte Carlo simulation. Here we compare the analytic approximations in (24) and (27) with Monte Carlo simulations, when the stochastic parametric excitation $\kappa(t)$, with mean m and standard deviation k, is given by an exponential squared correlation function of the form $R(\tau) = \exp(-\tau^2/2)$.

We solve (12) using the Euler–Mayaruma method [40] from $t_0 = 0$ to $t_f = 200$ with step size $\Delta t = 2^{-9}$. Realization of the Gaussian process $\kappa(t)$ is generated according to an exact time domain method [41]. To preform simulations we fix the following values for the system parameters: $\sigma_x = 0.75$, $m = 5.00$. For the results in this subsection, we furthermore fix the value of friction at $c = 0.38$, which corresponds to an average of one oscillation during the decay phase of an instability. Moreover, for this subsection, samples after 20 computational steps are stored and used in calculations, and 5000 realizations are used for $k = 1.8$ and 2500 realizations otherwise. In Figures 9, 10, and 11, Monte Carlo results for the pdf for position and velocity are compared with the analytic results given in (24) and (27), for various k values, which controls the mean number of instabilities for fixed m through the parameter η. Observe that the analytical pdf for position and velocity match the results from Monte Carlo simulations for both extreme events and the main stable response, capturing the overall shape and probability values accurately (the figures for position are plotted out to 50 standard deviations of the stable Gaussian core).

4.6.2. Parameters and region of validity. Here we quantify the effect of varying system parameters on our analytical approximations. In particular, we consider the effect of both friction c and the frequency of instabilities, controlled by η, on our results by computing the Kullback–Leibler (KL) divergence, which measures the relative information lost by using our approximate analytical pdf instead of the "true" pdf from Monte Carlo simulations.

For a more physical interpretation of the effect of the friction parameter, we instead consider the typical number of oscillations the system undergoes during the decay phase of an instability, i.e., the number of oscillations before the system returns back to the stable regime. To determine the value of damping in terms of the number of oscillations N during the decay phase, consider that in section 4.2 we derived the approximation (equation (18)) $T_{\text{inst}} = (1 + 2\overline{\Lambda}_{\kappa<0}/c)T_{\kappa<0}$, so that the duration of the decay phase is given by $T_{\text{decay}} =$

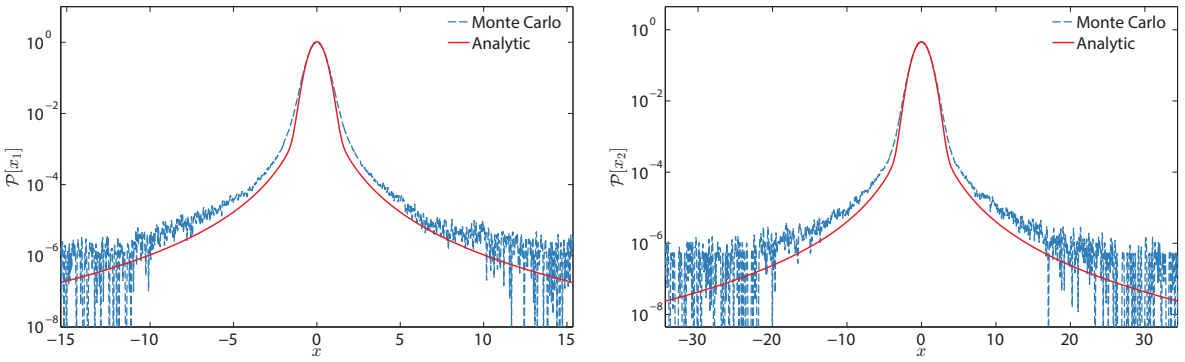

Figure 9. *Analytic pdfs* (24), (27) *compared with results from Monte Carlo simulations for position (left) and velocity (right), for parameters* $k = 1.8$, $m = 5.0$, $c = 0.38$, $\sigma_x = 0.75$.

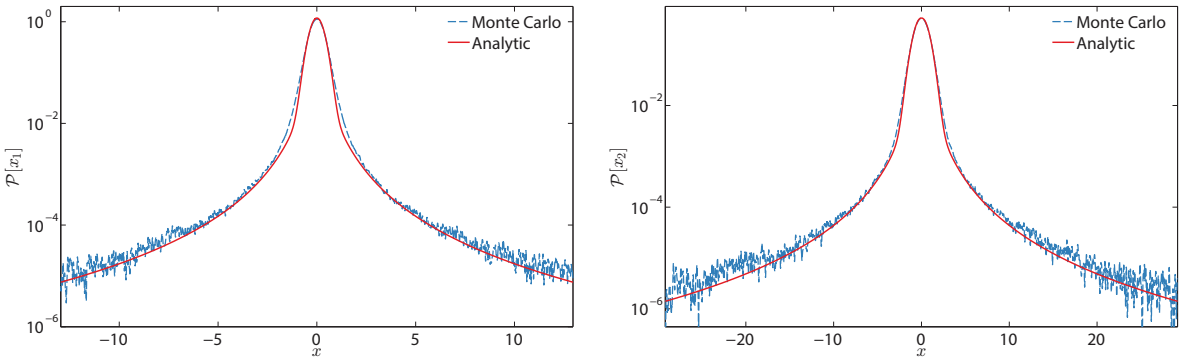

Figure 10. *Analytic pdfs* (24), (27) *compared with results from Monte Carlo simulations for position (left) and velocity (right), for parameters* $k = 2.2$, $m = 5.0$, $c = 0.53$, $\sigma_x = 0.75$.

$(2\overline{\Lambda}_{\kappa<0}/c)T_{\kappa<0}$. Thus, the average length of the decay phase is $\overline{T}_{\text{decay}} = (2\overline{\Lambda}_{\kappa<0}/c)\overline{T}$ (where $\overline{T}$ denotes the conditional average $\overline{T}_{\kappa<0}$), and the corresponding value of damping that will give on average N oscillations during the decay phase is therefore

$$N = \frac{\omega_s}{2\pi}\overline{T}_{\text{decay}} = \frac{\omega_s}{2\pi}\frac{2\overline{\Lambda}_{\kappa<0}}{c}\overline{T} \implies c = \frac{\omega_s \overline{\Lambda}_{\kappa<0}}{\pi N}\overline{T},$$

where $\overline{T}$ is given in (9) and ω_s in (13).

In Figure 12, we compute the KL divergence for a range of k and N parameter values. For the simulations we fix $m = 5.0$, store values after 40 computational steps, and use 4000 realizations for $k \leq 2.0$ and 2000 realizations, otherwise. In addition, we compute the divergence for every half oscillation number from $N = 0.5$ to $N = 3.0$ and every k value from $k = 1.4$ to $k = 3.6$, in increments of 0.2, and interpolate values in between. Overall, we have good agreement for a wide range of parameters, and even when the analytical results do not capture the exact probability values accurately, we have qualitative agreement with the overall shape of the pdf. The analytical results deviate when we are in regimes with very frequent instabilities and instabilities of long duration, i.e., small friction values or large N val-

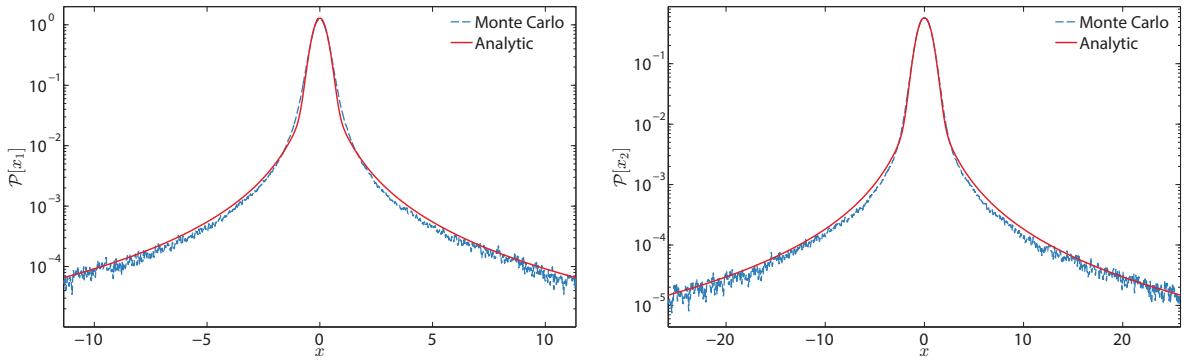

Figure 11. *Analytic pdfs* (24), (27) *compared with results from Monte Carlo simulations for position (left) and velocity (right), for parameters* $k = 2.6$, $m = 5.0$, $c = 0.69$, $\sigma_x = 0.75$.

ues. This is expected; in such regimes the instabilities are no longer statistically independent, which we assume in A1. Furthermore, an average of $N = 1$ oscillation during the decay phase shows good agreement with Monte Carlo results for a large range of frequency of instabilities parameter η.

We also observe that deviations of the analytical approximation from the Monte Carlo simulation become more prominent as k decreases. Note that for small k sampling the tails is very hard since the critical events occur very infrequently in this case. To understand the deviation of the analytical solution we recall that for this parametric regime the unstable region is characterized by rare events which are shorter and weaker and therefore harder to distinguish from the regular events. This explains the good analytical approximation properties as k increases (but not too large), where we have clear separation of the system behavior between the stable and the unstable regimes. Finally, we emphasize that the KL divergence may be (relatively) large despite the analytic pdf capturing the probabilities in the tails accurately; this is due to the fact that tail events are associated with extremely small probability values, which the KL divergence does not emphasize over the stable regime, where the probabilities are large and thus any deviations (e.g., due to a cusp) can heavily impact divergence values.

5. Application to an intermittently unstable complex mode. Here we present the second application of the method formulated in section 2 to that of a complex scalar Langevin equation that models a single mode in a turbulent signal, where multiplicative stochastic damping $\gamma(t)$ and colored additive noise $b(t)$ replace interactions between various modes. The nonlinear system is given by

$$\frac{du(t)}{dt} = (-\gamma(t) + i\omega)u(t) + b(t) + f(t) + \sigma\dot{W}(t), \tag{28}$$

where $u(t) \in \mathbb{C}$ physically describes a resolved mode in a turbulent signal and $f(t)$ is a prescribed deterministic forcing. The process $\gamma(t)$ models intermittency due to the (hidden) nonlinear interactions between $u(t)$ and other unobserved modes. In other words, intermittency in the variable $u(t)$ is primarily due to the action of $\gamma(t)$, with $u(t)$ switching between stable and unstable regimes when $\gamma(t)$ switches signs between positive and negative values.

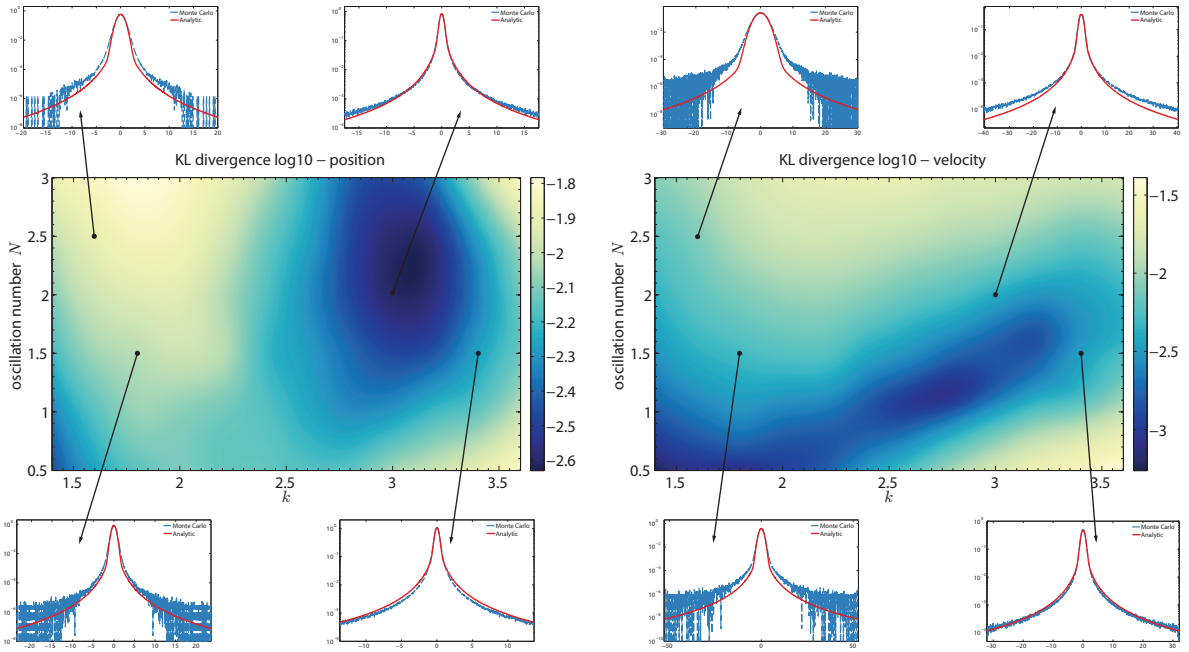

Figure 12. *KL divergence for position (left) and velocity (right) between analytic and Monte Carlo results for various values of damping (in terms of the number of oscillations N after an instability) and k, which controls the number of instabilities. For all cases $m = 5.0$.*

The nonlinear system (28) was introduced for filtering of multiscale turbulent signals with hidden instabilities [42, 43] and has been used extensively for filtering, prediction, and calibration of climatological systems [12, 44, 9, 10, 8]. This system features rich dynamics that closely mimic turbulent signals in various regimes of the turbulent spectrum. In particular, there are three physically relevant dynamical regimes of (28); the three regimes are described by [44] (and are reproduced here for completeness):

R1. This is a regime where the dynamics of $u(t)$ are dominated by frequent, short-lasting transient instabilities, which is characteristic of the dynamics in the turbulent energy transfer range.

R2. In this regime the dynamics of $u(t)$ are characterized by large-amplitude intermittent instabilities followed by a relaxation phase. Here the dynamics are characteristic of turbulent modes in the dissipative range.

R3. This regime is characterized by dynamics of $u(t)$ where transient instabilities are very rare and fluctuations in $u(t)$ rapidly decorrelate. This type of dynamics is characteristic of the laminar modes in the turbulent spectrum.

We apply the method described in section 2 to approximate the probability distribution for the dynamics of $u(t)$ in the special case with no additive noise, i.e., $b = 0$, and no external forcing $f = 0$. This is the simplest case that incorporates intermittency driven by parametric excitation process $\gamma(t)$ (the additive noise term $b(t)$ only impacts the strength of intermittent

events). The system we consider is given by

$$\frac{du(t)}{dt} = (-\gamma(t) + i\omega)u(t) + \sigma\dot{W}(t), \tag{29}$$

where intermittent events are triggered when $\gamma(t) < 0$. The parametric excitation process $\gamma(t)$ will be characterized by a mean m and variance k^2, so that $\eta \equiv -m/k$ represents the extreme event level, and also a time correlation length scale L. This application is a good test case of our method for the derivation of analytic approximations for the pdf of intermittent systems, since the dynamics of $u(t)$ are such that it oscillates at a fixed frequency ω, and therefore no approximations need to be made as in section 4 for the growth exponent in the unstable state. However, the Langevin equation has the difficulty that the nature of its interactions with the parametric excitation process introduces "instabilities" of such small magnitude that they are indistinguishable from the typical stable response, and so a clean separation must be enforced in the analysis of the unstable state. We present these differences and derive the system response pdf for the real/imaginary parts of the response $u = u_r + iu_i$, which statistically converge to the same distribution so that $\mathbb{P}(u_r)$ and $\mathbb{P}(u_i)$ are equivalent. We compare the analytical result for all three regimes R1–R3, but we note that the pdf in regime 3 is nearly Gaussian, so the full application of our method is excessive.

5.1. Probability distribution in the stable regime. Here we derive approximation of the pdf for $u(t)$ given that we are in the stable regime and, moreover, that we have statistical stationarity. In the stable regime, following section 2.1, we replace $\gamma(t)$ by the conditional average

$$\overline{\gamma}|_{\gamma>0} = m + k\frac{\phi(\eta)}{1-\Phi(\eta)}.$$

Thus the governing equation in the stable regime becomes

$$\frac{du(t)}{dt} = (-\overline{\gamma}|_{\gamma>0} + i\omega)u(t) + \sigma\dot{W}(t),$$

with the exact solution

$$u(t) = u(0)e^{(-\overline{\gamma}|_{\gamma>0}+i\omega)(t-t_0)} + \sigma\int_{t_0}^{t} e^{(-\overline{\gamma}|_{\gamma>0}+i\omega)(t-s)}\,dW(s).$$

Since this is a Gaussian system, we can fully describe the pdf for $u(t)$ in this regime by its stationary mean $\overline{u(t)} = 0$ and stationary variance

$$\mathrm{Var}(u(t)) = \mathrm{Var}(u_0)e^{-2\overline{\gamma}|_{\gamma>0}(t-t_0)} + \frac{\sigma^2}{2\overline{\gamma}|_{\gamma>0}}(1 - e^{-2\overline{\gamma}|_{\gamma>0}(t-t_0)}) \to \frac{\sigma^2}{2\overline{\gamma}|_{\gamma>0}} \quad \text{as } t\to\infty. \tag{30}$$

Therefore, we have the following pdf for the real part of $u(t)$ in the stable regime:

$$p_{u_r}(x \mid \text{stable}) = \sqrt{\frac{2\overline{\gamma}|_{\gamma>0}}{\pi\sigma^2}}\exp\left(-\frac{2\overline{\gamma}|_{\gamma>0}}{\sigma^2}x^2\right). \tag{31}$$

5.2. Probability distribution in the unstable regime. In the unstable regime, as in the previous application, we describe the probability distribution in terms of the envelope process. Following assumption A2, we ignore σ^2 in (29), which does not have a large probabilistic impact on the instability strength, so that the envelope of $u(t)$ is given by

$$\frac{du(t)}{dt} = (-\gamma(t) + i\omega)u(t) \implies \frac{d|u|^2}{dt} = 2\,\mathrm{Re}\left[\frac{du}{dt}u^*\right] = -2\gamma(t)|u|^2, \tag{32}$$

where $\square^*$ is the complex conjugate. Substituting the representation $|u| = e^{\Lambda T}$ into (32), we get $\Lambda = -\gamma$. Now since $\mathbb{P}(\Lambda) = \mathbb{P}(-\gamma \mid \gamma < 0)$, we have

$$p_\Lambda(\lambda) = \frac{1}{\Phi(\eta)} p_\gamma(-\lambda) = \frac{1}{k\Phi(\eta)}\phi\left(-\frac{\lambda + m}{k}\right), \quad \lambda > 0. \tag{33}$$

The conditionally unstable pdf will be exactly as in (16), with the minor modification that the distribution of the growth exponent is given instead by (33). Making this modification, we have the following pdf for the envelope in the unstable regime (where $\overline{T} = \overline{T}_{\gamma<0}$):

$$p_{|u|}(u \mid \gamma < 0, |u_0|) = \frac{\pi \log(u/u_0)}{2k\overline{T}^2\Phi(\eta)u}\int_0^\infty \frac{1}{y^2}\phi\left(-\frac{y+m}{k}\right)\exp\left(-\frac{\pi}{4\overline{T}^2 y^2}\log(u/u_0)^2\right)dy,\ u > u_0. \tag{34}$$

In addition, using (7), we have that the average length of an instability is given by

$$\frac{T_{\text{decay}}}{T_{\gamma<0}} = -\frac{m - k\frac{\phi(\eta)}{\Phi(\eta)}}{m + k\frac{\phi(\eta)}{1-\Phi(\eta)}} \equiv \mu \implies T_{\text{inst}} = (1-\mu)T_{\gamma<0}. \tag{35}$$

Finally, to construct the full distribution for the envelope of $u(t)$ in the unstable regime, we need to incorporate the distribution of the initial point of the instability, which is described by the envelope of $u(t)$ in the stable regime; in other words, $\mathbb{P}(|u| \mid \gamma < 0) = \mathbb{P}(|u| \mid \gamma < 0, |u_0|)\mathbb{P}(|u_0|)$. The pdf for the envelope of a general Gaussian process was described in section 4.3. However, as we noted in the introduction, the complex scalar Langevin equation has the property that its interaction with the parametric excitation gives rise to "instabilities" of very small intensity which are indistinguishable from the typical stable state response. To enforce the separation of the unstable response from the stable state requires us to introduce the following correction to the initial point of the instability $|u_0| = |\tilde{u}_0| + c$, where $|\tilde{u}_0|$ is the pdf of the envelope of the stable response (22) and c is a constant that enforces the separation. We find that choosing c such that it is one standard deviation of the typical stable response (equation (30)) is sufficient to enforce this separation and works well in practice. In addition, this choice is associated with very robust performance over different parametric regimes. Therefore, we have that the distribution of the initial point of an instability is given by

$$p_{|u_0|}(x) = \frac{4\overline{\gamma}|_{\gamma>0}}{\sigma^2}(x-c)\exp\left(-\frac{2\overline{\gamma}|_{\gamma>0}}{\sigma^2}(x-c)^2\right), \quad x > c. \tag{36}$$

As in section 4.2, we note that the oscillatory character during an instability has to be taken into account. However, to avoid the additional integral that would result should this

be taken into account by an additional random variable transformation, we instead utilize the same approximation

$$p_{u_r}(x \mid \gamma < 0) = \frac{1}{2} p_{|u|}(|x| \mid \gamma < 0). \tag{37}$$

We will show in the following sections that this approximation compares favorably with direct numerical simulations.

5.3. Summary of analytical results for the complex mode. Combining (31), (34), (36), and (35) into the total probability law decomposition (1) and utilizing the approximation (37) gives the following heavy-tailed, symmetric pdf for the complex mode $u(t) = u_r(t) + iu_i(t)$, for $x \in \mathbb{R}$:

$$p_{u_r}(x) = \big(1 - (1-\mu)\Phi(\eta)\big)\sqrt{\frac{2\overline{\gamma}|_{\gamma>0}}{\pi\sigma^2}}\exp\left(-\frac{2\overline{\gamma}|_{\gamma>0}}{\sigma^2}x^2\right) + (1-\mu)\frac{\sqrt{2\pi\overline{\gamma}}|_{\gamma>0}}{2\sigma^2 k\overline{T}^2} \cdot \int_c^{|x|}\int_0^{\infty} \frac{\log(|x|/u_0)}{y^2(|x|/(u_0-c))}\exp\left(-\frac{(y+m)^2}{2k^2} - \frac{\pi}{4\overline{T}^2 y^2}\log(|x|/u_0)^2 - \frac{2\overline{\gamma}|_{\gamma>0}}{\sigma^2}(u_0-c)^2\right) dy\, du_0, \tag{38}$$

where the integral is understood to be zero when $x < c$.

Note that in this case, we do not use an asymptotic expansion for the integral in the unstable regime due to the fact that the resulting expression does not agree as precisely as the integral expansion for the parametrically excited oscillator application. However, the resulting expansion does follow the same decay as the full integral; thus should an asymptotic expansion for the integral be sought, the derivation follows the description given in section 4.2.1

5.4. Comparisons with direct Monte Carlo simulations. Here we compare the analytic results (38) with direct Monte Carlo simulations in the three regimes R1–R3 described in the introduction of the current section. Monte Carlo simulations are carried by numerically discretizing the governing system (29) using the Euler–Mayaruma method with a time step $\Delta t = 10^{-4}$. We store results after 10 computational steps and use 500 ensembles of time length $t = 700$, discarding the first $t = 200$ time data to ensure steady state statistics, for the calculation of the kernel density estimate for the pdf. We prescribe the parametric excitation process to have an exponential squared time correlation function with a time length scale L, of the form $R(\tau) = \exp(-\tau^2/(2L))$, and simulate the Gaussian process directly from the correlation function.

In Figure 13, the results for regime 1 are presented alongside a sample realization. As previously mentioned, this regime is characterized by frequent short-lasting instabilities. We observe that the analytical results are able to capture the the heavy-tails of the response probability distribution accurately, including the Gaussian core. In contrast, in regime 2 (see Figure 14), we have large-amplitude instabilities that occur less frequently. Again the analytical results in this regime are able to capture the probability distribution of the response accurately. In both regimes 1 and 2, the pdf of the response is plotted out to 200 standard deviations of the stable state's standard deviation to show the remarkable agreement of the tails between the analytical solution and Monte Carlo results. In Figure 15 we present the results for regime 3 for completeness, even though, as previously mentioned, this regime is

nearly Gaussian and intermittent events occur very rarely, and under certain parameters almost surely no instabilities will be observed.

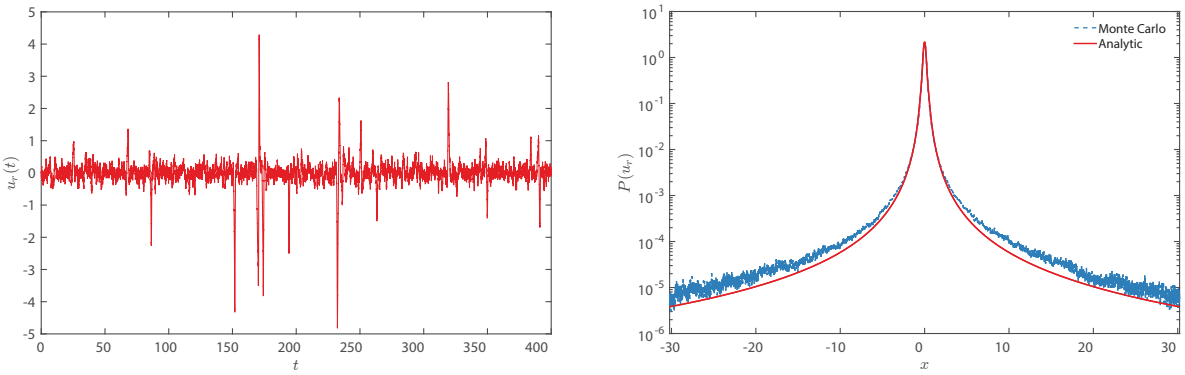

Figure 13. *Regime* 1: *Sample path (left) and analytic pdf* (38) *compared with results from Monte Carlo simulations (right), for parameters* $\omega = 1.78$, $\sigma = 0.5$, $m = 2.25$, $k = 2.0$, $L = 0.125$.

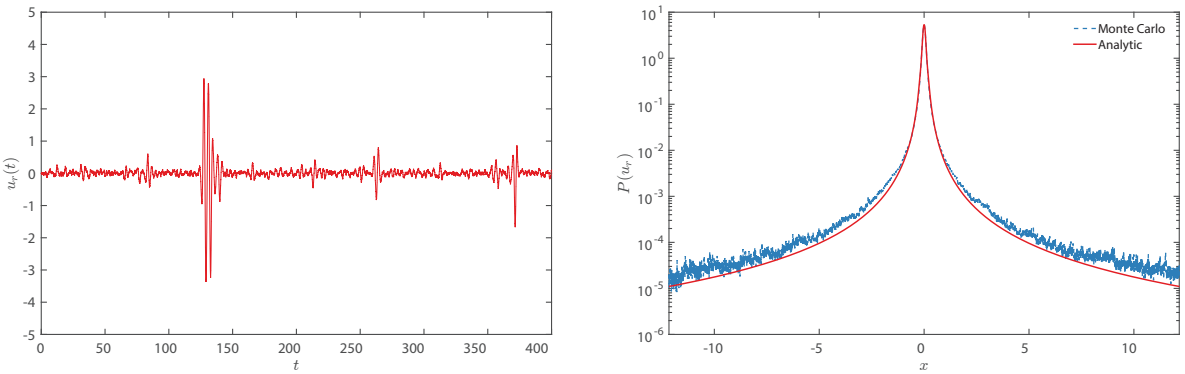

Figure 14. *Regime* 2: *Sample path (left) and analytic pdf* (38) *compared with results from Monte Carlo simulations (right), for parameters* $\omega = 1.78$, $\sigma = 0.1$, $m = 0.55$, $k = 0.50$, $L = 2.0$.

6. Conclusions and future work. We have formulated a general method to analytically approximate the pdf of intermittently unstable systems excited by correlated stochastic noise, under a set of assumptions applicable to a broad class of problems commonly encountered in engineering practice. The method developed in this paper relies on conditioning the system response on stable regimes and unstable events according to a total probability law argument and the reconstruction of the full probabilistic response after separate analysis of the conditional distributions in the two regimes. Thus, we have demonstrated how the system's response can be decomposed into a statistically stationary part (the stable regime) and an essentially transient part (the unstable regime). We have shown how this decomposition accurately captures the heavy-tail statistics that arise due to the presence of intermittent events in the dynamical system's response, providing a direct link between the character of

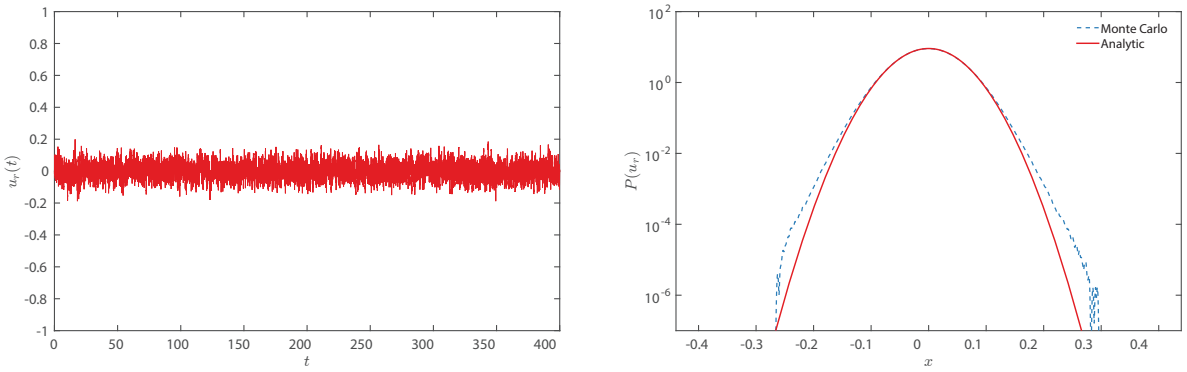

Figure 15. *Regime* 3: *Sample path (left) and analytic pdf* (38) *compared with results from Monte Carlo simulations (right), for parameters* $\omega = 1.78$, $\sigma = 0.25$, $m = 8.1$, $k = 1.414$, $L = 4.0$.

the intermittent instabilities and the form of the heavy-tail statistics of the response.

We have applied the formulated method on two prototype intermittently unstable systems: a mechanical oscillator excited by correlated multiplicative noise, and a complex mode that represents intermittent modes of a turbulent system. In both cases, our analytic approximations compare favorably with Monte Carlo simulations under a broad range of parameters. In the mechanical oscillator application, our analysis has furthermore unveiled that intermittency in velocity does not obey the familiar scaling of position with the stable state frequency, and that the conditionally unstable pdf must be scaled by a frequency that accounts for both the stable state frequency (fast) and a (slow) frequency associated with intermittent events. In this case, we have made appropriate approximations to account for this observation, and the resulting pdf compares well with direct simulations. In the complex mode application, we derived the system response pdf, and the analytical approximation compares well with Monte Carlo results for the three regimes commonly observed in turbulent signals.

Future work will include the extension of the method developed in this paper to the study of similar responses for more complex systems, involving more degrees of freedom. In particular, the research will be aimed at applying the developed technique for the probabilistic description of extreme events in ship rolling motion, in nonlinear water waves, and also in the motion of finite-sized particles in fluid flows.

Appendix. In this appendix we provide details regarding the asymptotic expansion of the integral in (17). According to Laplace's method, this integral will be distributed near the peak value of the term being exponentiated:

$$\theta(x, y; x_0) = -\frac{(y^2 + m)^2}{2k^2} - \frac{\pi}{4\overline{T}^2 y^2} \log(x/x_0)^2. \tag{39}$$

To find the maxima $y^* = \max_y \exp(\theta(x, y; x_0))$, we differentiate (39) with respect to y:

$$\frac{\partial \theta}{\partial y} = -2y\left(\frac{y^2}{k^2} + \frac{m}{k^2}\right) + \frac{\pi}{2\overline{T}^2 y^3} \log(x/x_0)^2.$$

To arrive at a closed form analytic approximation for y^*, we must determine the relative order of magnitude of y. To this end, investigating the terms in the integral in (16), we note that the maximum $y_{\max}$ of $p_\Lambda(y)$ will determine the order of magnitude of y,

$$\frac{d}{dy}p_\Lambda(y) = \frac{d}{dy}\left(\frac{2y}{k\Phi(\eta)\sqrt{2\pi}}\exp\left(-\frac{(y^2+m)^2}{2k^2}\right)\right) = 0 \implies 2y^4 + 2my^2 - k^2 = 0;$$

thus if $m^2 \gg k^2$, to leading order $y_{\max}^2 \simeq k^2/2m$ so that $y^2 \sim \mathcal{O}(k^2/m)$. Using this result, we may approximate (39) by

$$\frac{\partial\theta}{\partial y} \simeq 2y\frac{m}{k^2} + \frac{\pi}{2\overline{T}^2y^3}\log(x/x_0)^2 \implies y^*(x;x_0) = \left(\frac{\pi k^2}{4m\overline{T}^2}\right)^{1/4}\log(x/x_0)^{1/2}, \quad m^2 \gg k^2.$$

Acknowledgments. The authors thank Dr. Craig Merrill (NEEC Technical Point of Contact), Dr. Vadim Belenky, and Prof. Andrew Majda for numerous stimulating discussions.

REFERENCES

[1] J. Pedlosky, *Ocean Circulation Theory*, Springer-Verlag, New York, 1998.
[2] R. Salmon, *Lectures on Geophysical Fluid Dynamics*, Oxford University Press, Oxford, UK, 1998.
[3] T. DelSole, *Stochastic models of quasigeostrophic turbulence*, Surv. Geophys., 25 (2004), pp. 107–149.
[4] A. J. Majda, R. V. Abramov, and M. J. Grote, *Information Theory and Stochastics for Multiscale Nonlinear Systems*, CRM Monogr. Ser. 25, AMS, Providence, RI, 2005.
[5] A. J. Majda, D. W. McLaughlin, and E. G. Tabak, *A one-dimensional model for dispersive wave turbulence*, J. Nonlinear Sci., 6 (1997), pp. 9–44.
[6] K. Dysthe, H. Krogstad, and P. Muller, *Oceanic rogue waves*, in Annual Review of Fluid Mechanics, Annu. Rev. Fluid Mech. 40, Annual Reviews, Palo Alto, CA, 2008, pp. 287–310.
[7] W. Xiao, Y. Liu, G. Wu, and D. K. P. Yue, *Rogue wave occurrence and dynamics by direct simulations of nonlinear wave-field evolution*, J. Fluid Mech., 720 (2013), pp. 357–392.
[8] A. J. Majda and M. Branicki, *Lessons in uncertainty quantification for turbulent dynamical systems*, Discrete Contin. Dynam. Syst., 32 (2012), pp. 3133–3221.
[9] M. Branicki and A. J. Majda, *Quantifying uncertainty for predictions with model error in non-Gaussian systems with intermittency*, Nonlinearity, 25 (2012), pp. 2543–2578.
[10] A. J. Majda and J. Harlim, *Filtering Complex Turbulent Systems*, Cambridge University Press, Cambridge, UK, 2012.
[11] W. Cousins and T. P. Sapsis, *Quantification and prediction of extreme events in a one-dimensional nonlinear dispersive wave model*, Phys. D, 280 (2014), pp. 48–58.
[12] N. Chen, A. J. Majda, and D. Giannakis, *Predicting the cloud patterns of the Madden-Julian Oscillation through a low-order nonlinear stochastic model*, Geophys. Res. Lett., 41 (2014), pp. 5612–5619.
[13] A. H. Nayfeh and D. T. Mook, *Nonlinear Oscillations*, Wiley-Interscience, New York, 1984.
[14] H. W. Broer, I. Hoveijn, and M. van Noort, *A revertible bifurcation analysis of the inverted pendulum*, Phys. D, 112 (1997), pp. 50–63.
[15] D. Shadman and B. Mehri, *A non-homogeneous Hill's equation*, Appl. Math. Comput., 167 (2005), pp. 68–75.
[16] P. D. Kourdis and A. F. Vakakis, *Some results on the dynamics of the linear parametric oscillator with general time-varying frequency*, Appl. Math. Comput., 183 (2006), pp. 1235–1248.
[17] L. Arnold, I. Chueshov, and G. Ochs, *Stability and capsizing of ships in random sea—a survey*, Nonlinear Dynamics, 36 (2004), pp. 135–179.
[18] A. Babiano, J. H. Cartwright, O. Piro, and A. Provenzale, *Dynamics of a small neutrally buoyant sphere in a fluid and targeting in Hamiltonian systems*, Phys. Rev. Lett., 84 (2000), p. 5764.

[19] T. P. Sapsis and G. Haller, *Instabilities in the dynamics of neutrally buoyant particles*, Phys. Fluids, 20 (2008), 017102.
[20] G. Haller and T. P. Sapsis, *Localized instability and attraction along invariant manifolds*, SIAM J. Appl. Dyn. Syst., 9 (2010), pp. 611–633.
[21] J. C. Poggiale and P. Auger, *Impact of spatial heterogeneity on a predator-pray system dynamics*, C.R. Biol., 327 (2004), pp. 1058–1063.
[22] A. Naess and T. Moan, *Stochastic Dynamics of Marine Structures*, Cambridge University Press, Cambridge, UK, 2012.
[23] T. Soong and M. Grigoriu, *Random Vibration of Mechanical and Structural Systems*, PTR Prentice Hall, Upper Saddle River, NJ, 1993.
[24] A. Naess, *Extreme value estimates based on the envelope concept*, Appl. Ocean Res., 4 (1982), pp. 181–187.
[25] M. Nicodemi, *Extreme value statistics*, in Encyclopedia of Complexity and Systems Science E, Springer, New York, 2009, p. 3317.
[26] M. R. Leadbetter, G. Lindgren, and H. Rootzen, *Extremes and Related Properties of Random Sequences and Processes*, Springer, New York, 1983.
[27] R.-D. Reiss and M. Thomas, *Statistical Analysis of Extreme Values*, 3rd ed., Birkhäuser, Basel, 2007.
[28] P. Embrechts, C. Kluppelberg, and T. Mikosch, *Modeling Extremal Events*, Springer, New York, 2012.
[29] J. Galambos, *The Asymptotic Theory of Extreme Order Statistics*, Wiley Ser. Probab. Math. Statist., John Wiley & Sons, New York, 1978.
[30] E. Kreuzer and W. Sichermann, *The effect of sea irregularities on ship rolling*, Computing in Science and Engineering, 8 (2006), pp. 26–34.
[31] K. Sobczyk, *Stochastic Differential Equations*, Kluwer Academic Publishers, Dordrecht, The Netherlands, 1991.
[32] T. P. Sapsis and G. A. Athanassoulis, *New partial differential equations governing the joint, response-excitation, probability distributions of nonlinear systems, under general stochastic excitation*, Probab. Eng. Mech., 23 (2008), pp. 289–306.
[33] D. Venturi, T. P. Sapsis, H. Cho, and G. E. Karniadakis, *A computable evolution equation for the joint response-excitation probability density function of stochastic dynamical systems*, Proc. R. Soc. Lond. Ser. A Math. Phys. Eng. Sci., 468 (2012), pp. 759–783.
[34] I. F. Blake and W. C. Lindsey, *Level-crossing problems for random processes*, IEEE Trans. Inform. Theory, 19 (1973), pp. 295–315.
[35] M. F. Kratz, *Level crossings and other level functionals of stationary Gaussian processes*, Probab. Surv., 3 (2006), pp. 230–288.
[36] S. O. Rice, *Distribution of the duration of fades in radio transmission: Gaussian noise model*, Bell System Tech. J., 37 (1958), pp. 581–635.
[37] M. S. Longuet-Higgins, *On the joint distribution of the periods and amplitudes of sea waves*, J. Geophys. Res., 80 (1975), pp. 2688–2694.
[38] C. M. Bender and S. A. Orszag, *Advanced Mathematical Methods for Scientists and Engineers* I, reprint of the 1978 original, Springer-Verlag, New York, 1999.
[39] R. S. Langley, *On various definitions of the envelope of a random process.*, J. Sound Vibration, 105 (1986), pp. 503 – 512.
[40] D. J. Higham, *An algorithmic introduction to numerical simulation of stochastic differential equations*, SIAM Rev., 43 (2001), pp. 525–546.
[41] D. B. Percival, *Simulating Gaussian random processes with specified spectra*, Computing Sci. Statist., 24 (1992), pp. 534–538.
[42] B. Gershgorin, J. Harlim, and A. J. Majda, *Test models for improving filtering with model errors through stochastic parameter estimation*, J. Comput. Phys., 229 (2010), pp. 1–31.
[43] B. Gershgorin, J. Harlim, and A. J. Majda, *Improving filtering and prediction of spatially extended turbulent systems with model errors through stochastic parameter estimation*, J. Comput. Phys., 229 (2010), pp. 32–57.
[44] M. Branicki, B. Gershgorin, and A. J. Majda, *Filtering skill for turbulent signals for a suite of nonlinear and linear extended Kalman filters*, J. Comput. Phys., 231 (2012), pp. 1462–1498.